DALTON

Electron paramagnetic resonance study of the $S = \frac{1}{2}$ ground state of a radiolysis-generated manganese(III)–trimanganese(IV) form of $[Mn^{IV}_4O_6(bipy)_6]^{4+}$ (bipy = 2,2′-bipyridine). Comparison with the photosynthetic Oxygen Evolving Complex †

Geneviève Blondin,[a] Roman Davydov,[b] Christian Philouze,[a] Marie-France Charlot,[a] Stenbjörn Styring,[b] Björn Åkermark,[c] Jean-Jacques Girerd *,[a] and Alain Boussac [d]

[a] *Laboratoire de Chimie Inorganique, URA CNRS 420, Institut de Chimie Moléculaire d'Orsay, Université Paris-Sud, 91405 Orsay, France*
[b] *Department of Biochemistry, Chemical Center, University of Lund, PO Box 124, 22100 Lund, Sweden*
[c] *Department of Chemistry/Organic Chemistry, Royal Institute of Technology, S-100 44 Stockholm, Sweden*
[d] *Section de Bioénergétique, URA CNRS 2906, DCBM, CEA Saclay, 91191 Gif sur Yvette cedex, France*

γ-Ray irradiation at liquid nitrogen temperature of a dimethylformamide solution of the tetranuclear complex $[Mn^{IV}_4O_6(bipy)_6]^{4+}$ (bipy = 2,2′-bipyridine) allowed the generation of the first mixed-valence tetranuclear system containing Mn^{III} and Mn^{IV} ions and exhibiting a $S = \frac{1}{2}$ ground state. The X-band EPR spectrum of this tetranuclear system has been obtained. Simulations have been undertaken and the Mn hyperfine coupling tensors determined clearly show a $Mn^{III}Mn^{IV}_3$ composition for the EPR active species. A general approach for the analysis of the isotropic components of the Mn hyperfine tensors is presented in detail. This allowed the determination of the spin projection value for each Mn site. A three *J* coupling scheme assuming that the linear topology of the starting compound remains is able to reproduce these spin projection values if and only if the Mn^{III} ion is located at a terminal position in a N_4O_2 environment. The EPR signal of this $[Mn_4O_6(bipy)_6]^{3+}$ species is compared with the multiline signal observed in the S_2 state of the photosynthetic Oxygen Evolving Complex.

Dioxygen is produced in photosynthetic living systems by the Oxygen Evolving Complex (OEC) which contains a Mn_4 cluster the structure and function of which are still unknown.[1] The OEC stores four oxidizing equivalents, generated one per photon by the charge separation system P680. This allows the four-electron oxidation of two water molecules into dioxygen. The OEC goes through five states $S_0 \longrightarrow S_1 \longrightarrow S_2 \longrightarrow S_3 \longrightarrow S_4$. The index corresponds to the number of oxidizing equivalents stored. It has been proposed that on the $S_2 \longrightarrow S_3$ step, a ligand instead of a Mn atom may be oxidized.[2] Dioxygen is evolved on the transition $S_4 \longrightarrow S_0$. The entry of water and exit of protons are difficult problems which have been studied. Messinger *et al.*[3] found that addition of ^{18}O water to OEC in the S_3 state led to the formation of principally $^{18}O^{16}O$. They suggested that dioxygen originates from one water molecule not directly bound to the manganese center and one terminal manganese oxo ligand. As far as protons are concerned, an attractive hypothesis is that on each step a proton be released in order to avoid an increase of the effective charge of OEC. Along the same line, a $H^{\bullet}$ abstraction has been proposed on each step.[4]

Extensive extended X-ray absorption fine structure (EXAFS) studies converge towards a description of OEC as being made up of two $[Mn_2O_2]$ moieties linked together in a not yet completely established mode.[1] A mono(oxo) bis(carboxylato) bridge has been proposed from EXAFS by analogy with known model complexes.[1]

The S_2 state of OEC gives a multiline EPR signal centred at $g = 2$.[5] It has been proposed from an analysis of the total width of this signal that it arises from a spin doublet state from a magnetic tetranuclear species.[6] A dinuclear origin has also been proposed.[7] This spectrum has been simulated with isotropic parameters[6,8] or with anisotropic ones.[9] Manganese-55 electron nuclear double resonance (ENDOR) transitions in OEC were observed in a narrower range (70–180 MHz) than those (90–280 MHz) in the $[Mn_2^{III,IV}O_2(bipy)_4]^{3+}$ (bipy = 2,2′-bipyridine) complex.[10] This would suggest that in OEC the absolute values of the hyperfine parameters are closer to each other than those for dinuclear systems. The consequence is that absolute values of the spin projections on Mn atoms in OEC seem closer to each other than in $[Mn^{III}Mn^{IV}O_2]^{3+}$ systems where they correspond to $\langle \boldsymbol{S}_{Mn^{III}z} \rangle = +1$ and $\langle \boldsymbol{S}_{Mn^{IV}z} \rangle = -0.5$.[11,12] The same ENDOR work[10] has questioned a dinuclear origin for the multiline signal.

A general agreement on the tetranuclear nature of the OEC seems to have been reached. Some disagreement remains on the oxidation level of the S_2 state. Basically the X-ray absorption near-edge structure (XANES) studies are in favour of a III,IV_3 distribution.[1] From EPR simulations using anisotropic hyperfine couplings, Zheng and Dismukes[9] propose a III_3,IV distribution.

Examples of EPR spectra of $S = \frac{1}{2}$ Mn tetranuclear species are needed to compare with that of OEC. To date, no artificial tetranuclear cluster has been reported with Mn in the +III and +IV oxidation states and a $S = \frac{1}{2}$ ground state.

It has been shown by one of us that γ-irradiation of $Fe^{III}Fe^{III}$ species leads to $Fe^{II}Fe^{III}$ mixed-valence species.[13] We show here that it is possible to produce at 77 K an EPR active $Mn^{III}Mn^{IV}_3$ cluster in a $S = \frac{1}{2}$ ground state by reduction of $[Mn^{IV}_4O_6(bipy)_6]^{4+}$ at 77 K with mobile electrons induced by ionizing γ-radiation.[13] We report here its EPR spectrum and compare it with the multiline signal from OEC.

† Based on the presentation given at Dalton Discussion No. 2, 2nd–5th September 1997, University of East Anglia, UK.

Non-Si unit employed: rad = 0.01 Gy.

Experimental

Syntheses

The complexes $[Mn_2O_2(phen)_4][ClO_4]_4\cdot 2H_2O$ **1** (phen = 1,10-phenanthroline)[14] and $[Mn_4O_6(bipy)_6][ClO_4]_4\cdot 2H_2O$ **2**[15] have been prepared according to published procedures.

Sample preparation

Complexes were dissolved in dimethylformamide (dmf) to form 3–5 mM solutions. Owing to the low stability of complex **2** in dmf the solution was immediately transferred into a 3 mm internal diameter quartz EPR tube and frozen. Solutions of complexes **1** and **2** in dmf or 30–35 mg of microcrystalline powder of the complexes in a quartz tube were irradiated by ^{137}Cs γ-rays while immersed in liquid nitrogen. Total irradiation doses were from 3–4.5 Mrad unless otherwise noted.

EPR measurements

The EPR spectra were recorded using a Bruker ESP 380e spectrometer with an Oxford Instrument 9 liquid helium cryostat. A strong EPR signal from free radicals induced by radiolysis centred at $g = 2.0$ overlaps with and distorts the mixed-valent EPR spectrum from the manganese cluster. To decrease contribution of the radical signal, the irradiated samples of the complexes **1** and **2** in dmf were annealed at 145–160 K for 3–5 min before such measurements.

After annealing at 160 K, the radical signal disappears whereas the signal from the mixed-valent species does not change. This signal starts markedly to decrease after annealing at $T > 190$ K.

EPR simulations

Simulation of EPR spectra was performed using a FORTRAN program originally developed by Drs. L. K. White and R. L. Belford at University of Illinois. The program simulates powder spectra for $S = \frac{1}{2}$ systems and can include four different hyperfine interactions using perturbation theory. It was modified to allow for calculation of the hyperfine contributions to the spectra to the second order.[6] Briefly, for each transition, the resonant field was calculated using perturbation theory up to the second order for the hyperfine coupling terms, and the resulting stick spectrum was then convoluted with Gaussian functions.

Results and Discussion

Production of III,IV states by radiolysis

The $[Mn^{IV}_2O_2(phen)_4]^{4+}$ complex is known to form a stable mixed-valent $Mn^{III,IV}$[16] state and was used to test the possibility of radiolytic one-electron reduction of polynuclear manganese complexes at 77 K. Previously radiolytic reduction has been successively applied for the generation and spectroscopic studies of various unstable dinuclear iron(II,III) centres.[13,17]

Fig. 1 shows EPR spectra from mixed-valent species produced by radiolytic reduction at 77 K of $[Mn^{IV}_2O_2(phen)_4]^{4+}$ in dmf [Fig. 1(*a*)] and from a chemically prepared sample of $[Mn^{III,IV}_2O_2(phen)_4]^{3+}$ [Fig. 1(*b*)]. These spectra are almost identical.

We previously reported the synthesis of a Mn^{IV} tetranuclear cluster $[Mn^{IV}_4O_6(bipy)_6]^{4+}$ the structure of which is shown in Fig. 2.[15] It has a linear topology with Mn ions grouped in pairs which are bridged by two oxo ions. The bond distances are Mn_a–Mn_b 2.746 Å, Mn_b–Mn_c 2.760 Å and Mn_c–Mn_d 2.735 Å. The topology is identical to the structural model for OEC proposed by Yachandra *et al.*[18] from EXAFS data. The Mn_b–Mn_c link is shorter in $[Mn^{IV}_4O_6(bipy)_6]^{4+}$ than in the OEC model previously mentioned where it is proposed to be a $Mn_bO(RCO_2)_2Mn_c$ unit with a 3.3 Å Mn–Mn separation.

Magnetic susceptibility measurement[15] on $[Mn^{IV}_4O_6(bipy)_6]^{4+}$ allowed the determination of $J_{ab} = J_{cd} = -176$ cm^{-1} and $J_{bc} = -268$ cm^{-1}. The ground state has a $S = 0$ electronic spin. The spin ordering in the ground state can be represented by alternate up and down spins.

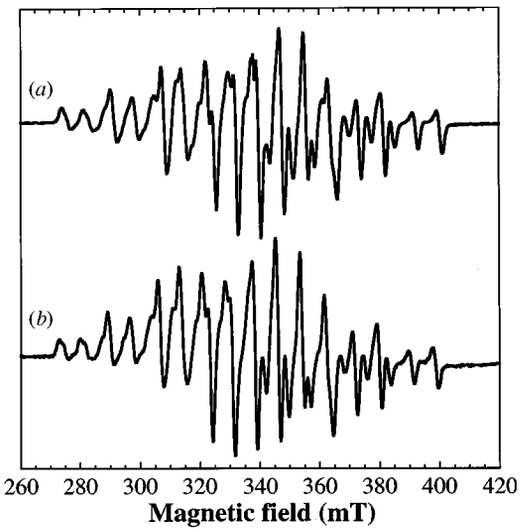

Fig. 1 X-Band EPR spectra of (*a*) a dmf solution of $[Mn^{IV}_2O_2(phen)_4]^{4+}$ γ-irradiated at 77 K and annealed at 190 K; (*b*) a dmf solution of a chemically prepared sample of $[Mn^{III,IV}_2O_2(phen)_4]^{3+}$. Conditions for spectrum (*a*): modulation frequency 100 kHz, modulation amplitude 0.5 mT, frequency 9.478 GHz, microwave power 0.92 mW, $T = 28$ K. Conditions for spectrum (*b*): modulation frequency 100 kHz, modulation amplitude 0.1 mT, frequency 9.4236 GHz, microwave power 52 μW, $T = 6.6$ K

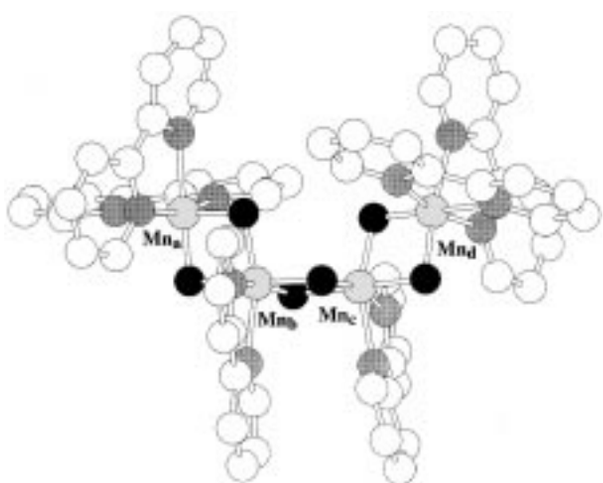

Fig. 2 Structure of $[Mn^{IV}_4O_6(bipy)_6]^{4+}$ showing the manganese atom labeling scheme. Hydrogen atoms are omitted

The cyclovoltammogram of $[Mn^{IV}_4O_6(bipy)_6]^{4+}$ exhibits an irreversible reduction wave. Attempts at reduction by electrolysis ended up with the decomposition of the tetranuclear complex into four Mn^{II} ions.[15] We have failed to prepare a monoreduced form, $[Mn^{III}Mn^{IV}_3O_6(bipy)_6]^{3+}$, by standard chemical reduction in solution.

By contrast, cryogenic radiolytic reduction allowed the production of an EPR active species. Fig. 3(*b*) shows an EPR spectrum from a solution of the tetranuclear manganese complex in dmf exposed to γ-radiation at 77 K. It contains 26 major lines centred at $g = 2$ and we will show that it might be assigned to a $[Mn^{III}Mn^{IV}_3O_6(bipy)_6]^{3+}$ species in the $S = \frac{1}{2}$ ground state with an electron localized on one of the manganese atoms.

The spectrum intensity increases linearly with irradiation dose up to 4.5 Mrad and levels off at doses higher than 6.5 Mrad. The lineshape of the multiline spectrum was independent of irradiation dose up to 6.5 Mrad. This observation implies that EPR active species trapped by cryogenic reduction is a

Table 1 Parameters obtained for the simulation of the EPR spectrum of $[Mn^{III}Mn^{IV}_3O_6(bipy)_6]^{3+}$

Symmetry	Isotropic	Axial	Rhombic
Number of parameters	5	10	15
Agreement factor R*	0.52	0.21	0.13
[g]			x 2.002
		⊥ 2.02	y 1.991
		∥ 1.99	z 1.987
g_{iso}	2.00	2.009	1.993
[A_1]/MHz			x 463.5
		⊥ 497	y 408.1
		∥ 321	z 476.0
$\|A_1^{iso}\|$/MHz	444	438.6	449.2
[A_2]/MHz			x 232.3
		⊥ 229	y 226.9
		∥ 242	z 225.8
$\|A_2^{iso}\|$/MHz	222	233.4	228.3
[A_3]/MHz			x 196.6
		⊥ 205	y 189.5
		∥ 225	z 182.1
$\|A_3^{iso}\|$/MHz	207	212.1	189.4
[A_4]/MHz			x 178.1
		⊥ 189	y 169.5
		∥ 192	z 166.9
$\|A_4^{iso}\|$/MHz	174	190.2	171.5

* The agreement factor R is calculated according to $\Sigma_i (y_i^{exp} - y_i^{calc})^2/\Sigma_i (y_i^{exp})^2$.

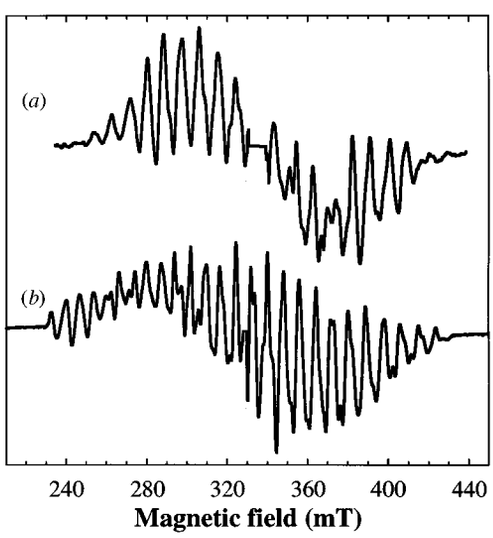

Fig. 3 Comparison of the X-band EPR spectra of OEC (*a*) and of $[Mn^{III}Mn^{IV}_3O_6(bipy)_6]^{3+}$ (*b*). Conditions for spectrum (*a*): modulation frequency 100 kHz, modulation amplitude 1.9 mT, frequency 9.421 GHz, microwave power 20 mW, $T = 10$ K. Conditions for spectrum (*b*): modulation frequency 100 kHz, modulation amplitude 0.3 mT, frequency 9.241 GHz, microwave power 20 mW, $T = 30$ K

monoreduced $Mn^{III}Mn^{IV}_3$ rather than a $Mn^{III}_3Mn^{IV}$ species. A monoreduced tetranuclear manganese cluster with an identical EPR spectrum may be also produced by γ-irradiation of microcrystalline powder at 77 K. However in this case the relative yield of the mixed-valent species was a factor of 10 lower than that in frozen solution. In addition, in irradiated microcrystalline samples, the free radical signal centred at $g = 2.0$ was observed to be much more stable than in dmf solution and decayed after annealing at $T > 190$ K together with the multiline mixed-valent signal. Therefore, the majority of the spectroscopic studies were carried out on solutions of the manganese complex in dmf.

We have found that the mixed-valent species giving rise to the multiline EPR spectrum of Fig. 3(*b*) was stable upon annealing of the irradiated sample at 180 K for 3 min. It quite rapidly disappeared at $T > 190$ K. Approximate quantitation of the signal of Fig. 3(*b*) *versus* 1 mM $Cu(ClO_4)_2$ standard indicates

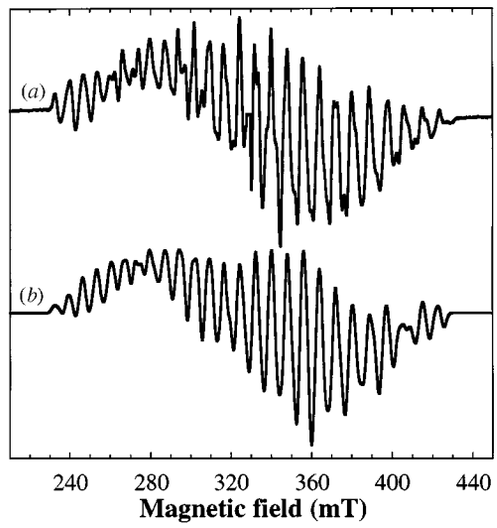

Fig. 4 Comparison of (*a*) the X-band EPR spectrum of $[Mn^{III}Mn^{IV}_3O_6(bipy)_6]^{3+}$ and (*b*) its best simulation corresponding to the rhombic parameters given in Table 1

that about 30% of the manganese complexes are in a mixed-valent state.

The lineshape of the multiline spectrum of Fig. 3(*b*) is independent of temperature between 4 and 60 K and of microwave power. At 77 K the signal is slightly broadened. This suggests that we are indeed observing a ground state well separated from the first excited state.

Simulations

Several simulations of the X-band EPR signal of $[Mn^{III}Mn^{IV}_3O_6(bipy)_6]^{3+}$ were obtained. The values of the parameters are shown in Table 1. An isotropic simulation was obtained using five isotropic tensors: $g = 2.00$, $|A_1| = 444$ MHz, $|A_2| = 222$ MHz, $|A_3| = 207$ MHz, $|A_4| = 174$ MHz. In all simulations a linewidth equal to 1.5 mT was used. Here, numbers 1–4 are used to refer to the manganese centers and not letters a–d as in the description of the structure. At this stage of the discussion no correlation is made between the two types of index. An axial simulation was also obtained (Table 1). An interesting feature of this simulation is that only the tensor corresponding to the largest hyperfine coupling has significant anisotropy. The perpendicular value $|A_{1\perp}| = 497$ MHz is found to be larger than the parallel one $|A_{1\|}| = 321$ MHz as is usual with six-co-ordinate elongated Mn^{III} ions.[11,12] This can be compared to the anisotropy found around Mn^{III} in $[Mn_2O_2(bipy)_4]^{3+}$ $|A_{1\perp}| = 490.5$ MHz, $|A_{1\|}| = 378$ MHz.[11] This clearly identifies the Mn_1 atom in $[Mn^{III}Mn^{IV}_3O_6(bipy)_6]^{3+}$ as Mn^{III}. A fully rhombic simulation was obtained (Table 1 and Fig. 4). This simulation is the best we could obtain from the large number tried; it gives the best agreement factor. Again only one tensor exhibits a large anisotropy and a large isotropic coupling value. The isotropic values are $|A_1| = 449.2$ MHz, $|A_2| = 228.3$ MHz, $|A_3| = 189.4$ MHz, $|A_4| = 171.5$ MHz, similar to those obtained in the isotropic fit. The values for the Mn_1Mn_2 pair are strongly reminiscent of those observed in $Mn^{III}Mn^{IV}$ dimers. For instance, for $[Mn_2O_2(bipy)_4]^{3+}$ $|A_1| = 453$ MHz, $|A_2| = 218.7$ MHz,[11] and for $[Mn_2O_2(L)_2]^{3+}$ (L = *N*,*N*′-bis(imidazol-4-ylmethyl)-*N*,*N*′-dimethylethane-1,2-diamine) $|A_1| = 456$ MHz, $|A_2| = 215$ MHz.[12]

Spin coupling analysis of a linear $Mn^{III}Mn^{IV}_3$ system with localized valences

We propose now a strategy to interpret these hyperfine isotropic coupling parameters. This strategy could be of general use.

The spin projection values $\langle \boldsymbol{S}_{iz} \rangle$ are related to the isotropic part of the hyperfine couplings A_i in the $S = \frac{1}{2}$ state through relation (1), where a_i is the isotropic part of the intrinsic hyper-

$$A_i = 2a_i \langle \boldsymbol{S}_{iz} \rangle \quad (1)$$

Table 2 Calculated spin projection $\langle S_{iz}\rangle$ values for a $Mn^{III}Mn^{IV}_3$ complex with a symmetry high enough in order that the spins S_{12} and S_{34} of the two pairs of coupled spins S_1, S_2 and S_3, S_4 respectively be good quantum numbers

$\lvert S_{12},S_{34},S\rangle$	$\langle S_{1z}\rangle$ Mn^{III}	$\langle S_{2z}\rangle$ Mn^{IV}	$\langle S_{2z}\rangle$ Mn^{IV}	$\langle S_{4z}\rangle$ Mn^{IV}
$\lvert 7/2,3,1/2\rangle$	+6/7	+9/14	−1/2	−1/2
$\lvert 5/2,3,1/2\rangle$	−11/21	−13/42	+2/3	+2/3
$\lvert 5/2,2,1/2\rangle$	+11/15	+13/30	−1/3	−1/3
$\lvert 3/2,2,1/2\rangle$	−2/5	−1/10	+1/2	+1/2
$\lvert 3/2,1,1/2\rangle$	+2/3	+1/6	−1/6	−1/6
$\lvert 1/2,1,1/2\rangle$	−1/3	+1/6	+1/3	+1/3
$\lvert 1/2,0,1/2\rangle$	+1	−1/2	0	0

fine coupling. We used for a_i the values deduced by Zheng *et al.*[11] for $[Mn_2O_2(bipy)_4]^{3+}$: $|a_{III}| = 227$ MHz, $|a_{IV}| = 219$ MHz. Thus we obtained the absolute values $|\langle S_{iz}\rangle|$, assuming that the largest $|A_i|$ belongs to Mn^{III}.

In a next step, we were able to attribute signs to those $\langle S_{iz}\rangle$ by choosing such a distribution of signs that the condition $\Sigma_i \langle S_{1z}\rangle = 0.5$ be obeyed. We obtained $\langle S_{1z}\rangle = +0.989$ (Mn^{III}), $\langle S_{2z}\rangle = -0.521$, $\langle S_{3z}\rangle = +0.432$, $\langle S_{4z}\rangle = -0.392$ which gives $\Sigma_i \langle S_{iz}\rangle = +0.508$. Other combinations give much poorer agreement. We have thus transformed the hyperfine coupling information in a set of $\langle S_{iz}\rangle$ values. We will now try to relate these values to a spin coupling scheme in this artificial tetramer.

In $Mn^{III}Mn^{IV}$ dimers in the $S = \frac{1}{2}$ state, the spin projections are independent of the J coupling and are given by the vectorial coupling scheme: $\langle S_{III_z}\rangle = +1$ and $\langle S_{IV_z}\rangle = -0.5$. In the tetramer, if the symmetry is high enough, two subspins can be good quantum numbers and then the spin projections are not directly related to the values of the J constants. If site 1 is a Mn^{III} ion, the other three being Mn^{IV}, the basis functions are obtained by coupling spins by pair, that is using spin operators $\boldsymbol{S}_{12} = \boldsymbol{S}_1 + \boldsymbol{S}_2$ and $\boldsymbol{S}_{34} = \boldsymbol{S}_3 + \boldsymbol{S}_4$, and then coupling the two subspins to get the total S according to $\boldsymbol{S} = \boldsymbol{S}_{12} + \boldsymbol{S}_{34}$. The four spin operators are then given by the vector coupling scheme shown in equations (2)–(5).

$$S_1 = \frac{\langle S_1 \cdot S_{12}\rangle}{\langle S_{12} \cdot S_{12}\rangle} \times \frac{\langle S_{12} \cdot S\rangle}{\langle S \cdot S\rangle} S \quad (2)$$

$$S_2 = \frac{\langle S_2 \cdot S_{12}\rangle}{\langle S_{12} \cdot S_{12}\rangle} \times \frac{\langle S_{12} \cdot S\rangle}{\langle S \cdot S\rangle} S \quad (3)$$

$$S_3 = \frac{\langle S_3 \cdot S_{34}\rangle}{\langle S_{34} \cdot S_{34}\rangle} \times \frac{\langle S_{34} \cdot S\rangle}{\langle S \cdot S\rangle} S \quad (4)$$

$$S_4 = \frac{\langle S_4 \cdot S_{34}\rangle}{\langle S_{34} \cdot S_{34}\rangle} \times \frac{\langle S_{34} \cdot S\rangle}{\langle S \cdot S\rangle} S \quad (5)$$

One can calculate the four spin projection values[5] as shown in equations (6)–(9). The possible values for a $Mn^{III}Mn^{IV}_3$

$$\langle S_{1z}\rangle = \frac{S_{12}(S_{12}+1) + S_1(S_1+1) - S_2(S_2+1)}{2\,S_{12}(S_{12}+1)} \times \frac{S(S+1) + S_{12}(S_{12}+1) - S_{34}(S_{34}+1)}{2\,S(S+1)} \langle S_z\rangle \quad (6)$$

$$\langle S_{2z}\rangle = \frac{S_{12}(S_{12}+1) + S_2(S_2+1) - S_1(S_1+1)}{2\,S_{12}(S_{12}+1)} \times \frac{S(S+1) + S_{12}(S_{12}+1) - S_{34}(S_{34}+1)}{2\,S(S+1)} \langle S_z\rangle \quad (7)$$

$$\langle S_{3z}\rangle = \frac{S_{34}(S_{34}+1) + S_3(S_3+1) - S_4(S_4+1)}{2\,S_{34}(S_{34}+1)} \times \frac{S(S+1) + S_{34}(S_{34}+1) - S_{12}(S_{12}+1)}{2\,S(S+1)} \langle S_z\rangle \quad (8)$$

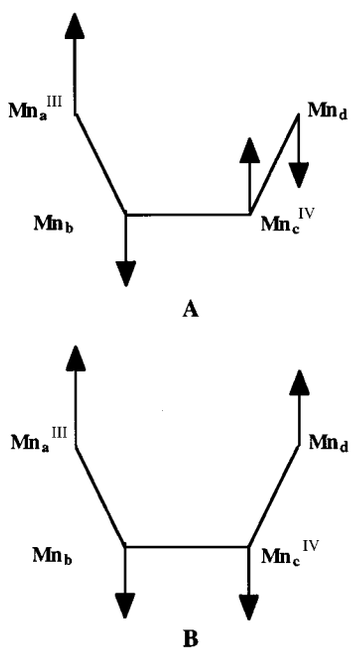

Scheme 1

$$\langle S_{4z}\rangle = \frac{S_{34}(S_{34}+1) + S_4(S_4+1) - S_3(S_3+1)}{2\,S_{34}(S_{34}+1)} \times \frac{S(S+1) + S_{34}(S_{34}+1) - S_{12}(S_{12}+1)}{2\,S(S+1)} \langle S_z\rangle \quad (9)$$

tetramer for each of the seven $|S_{12},S_{34},S = \frac{1}{2}\rangle$ states are obtained using $\langle S_z\rangle = 0.5$ in the preceding formula and are given in Table 2. We see that no $|S_{12},S_{34},S = \frac{1}{2}\rangle$ gives a set of $\langle S_{iz}\rangle$ values approaching the experimental one. We will now show that this is in agreement with a retention, after irradiation, of a linear topology for this $Mn^{III}Mn^{IV}_3$ system.

The following spin Hamiltonian [equation (10)] is adapted to

$$H = -J_{ab}S_aS_b - J_{bc}S_bS_c - J_{cd}S_cS_d \quad (10)$$

a four-spin coupling problem with a linear topology. Letters are employed as indexation of the manganese centers since here we refer to the structure of the tetranuclear complex $[Mn^{IV}_4O_6(bipy)_6]^{4+}$. As already stressed in our study of the Mn^{IV} tetramer[15] no analytical solution exists for this apparently simple spin coupling problem. The only good quantum numbers are S and M_S except for some particular values of the exchange constants which allow additional quantum numbers.

The fact that with such a simple topology the ground state has $S = \frac{1}{2}$ for $J_{ab} < 0$, $J_{bc} < 0$, $J_{cd} < 0$ can be illustrated as in Scheme 1 **A** with Mn^{III} on site a. When one has $J_{ab} < 0$, $J_{bc} > 0$, $J_{cd} < 0$, the ground state still has $S = \frac{1}{2}$ as indicated in Scheme 1 **B**. This is also the case if the Mn^{III} ion is on site b. With such a

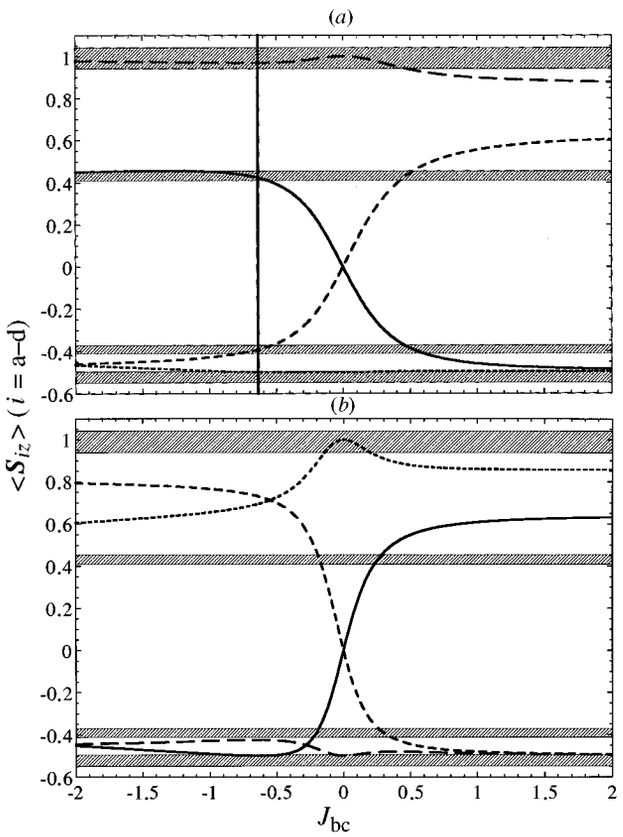

Fig. 5 Calculated spin projection $\langle \boldsymbol{S}_{iz} \rangle$ values for a $Mn_aMn_bMn_cMn_d$ linear complex with a three J coupling scheme, as a function of J_{bc}, J_{ab} and J_{cd} are kept equal to -1 in arbitrary units (see Hamiltonian in the text). The oxidation state is $Mn^{III}Mn^{IV}{}_3$. (——) $\langle \boldsymbol{S}_{az} \rangle$, (- - -) $\langle \boldsymbol{S}_{bz} \rangle$, (——) $\langle \boldsymbol{S}_{cz} \rangle$, (– – –) $\langle \boldsymbol{S}_{dz} \rangle$. The four hatched zones represent the experimentally determined $\langle S_{iz} \rangle$ values with a ±5% allowance; $J_{bc} = 0$ corresponds to two independent dimers, a $Mn_a{}^{III}Mn_b{}^{IV}$ and a $Mn_c{}^{IV}Mn_d{}^{IV}$ (see text). (*a*) Mn^{III} on site a ($J_{bc} = -0.64$) and (*b*) Mn^{III} on site b. The vertical line in (*a*) corresponds to the solution $J_{bc} = -0.64$

topology the $\langle \boldsymbol{S}_{iz} \rangle$ do not correspond to the values in Table 2 and they have to be computed using irreducible tensor methods.

We have solved the general problem of four electronic spins S_i (i = a or d) interacting *via* six exchange coupling constants J_{ij} (i,j = a, d) where S and M_S are the only good quantum numbers [equation (11)].

$$H = -\sum_{i<j} J_{ij} \boldsymbol{S}_i \cdot \boldsymbol{S}_j \qquad (11)$$

The ground state function $|\Psi\rangle$ is a linear combination of the basis functions $|S_{ab}, S_{cd}, S\rangle$ [equation (12)] where the c_k coefficients depend upon the exchange coupling constants. One can then calculate the spin projection values $\langle \boldsymbol{S}_{iz} \rangle = \langle \Psi | \boldsymbol{S}_{iz} | \Psi \rangle$ using irreducible tensor theory.[19] Here we apply this procedure to the particular case where $J_{ac} = J_{ad} = J_{bd} = 0$. Before calculating the spin projection values, we systematically verify that the ground state function belongs to the $S = \frac{1}{2}$ subspace.

$$|\Psi\rangle = \sum_k c_k |S_{12}, S_{34}, S\rangle \qquad (12)$$

Fig. 5(*a*) represents the calculated $\langle \boldsymbol{S}_{iz} \rangle$ values for the $S = \frac{1}{2}$ ground state as a function of J_{bc} with the hypotheses $J_{ab} = J_{cd} = -1$ (arbitrary units) and Mn^{III} on site a (terminal). When the magnetic connection between the two Mn_2O_2 dimers is zero, one evidently finds for the $Mn^{III}O_2Mn^{IV}$ dinuclear moiety the usual values $\langle \boldsymbol{S}_{IIIz} \rangle = +1$ and $\langle \boldsymbol{S}_{IVz} \rangle = -0.5$ and for the $Mn^{IV}O_2Mn^{IV}$ entity, $\langle \boldsymbol{S}_{IVz} \rangle = 0$. The spin density is concentrated on the III,IV dimer. When a magnetic connection is built between the two MnO_2Mn entities, spin density appears on sites c and d without affecting very much sites a and b. When the J_{bc} connection is antiferromagnetic, we note that $\langle \boldsymbol{S}_{az} \rangle$ (this is the Mn^{III} ion) stays close to +1 and that $\langle S_{bz} \rangle$ is close to −0.5. Moreover $\langle \boldsymbol{S}_{cz} \rangle$ is positive and $\langle \boldsymbol{S}_{dz} \rangle$ is negative. When the J_{bc} connection is strongly ferromagnetic, the limit values are $\langle \boldsymbol{S}_{az} \rangle = +12/14$, $\langle \boldsymbol{S}_{bz} \rangle = -1/2$, $\langle \boldsymbol{S}_{cz} \rangle = -1/2$, $\langle \boldsymbol{S}_{dz} \rangle = +9/14$. Those values are identical with those which can be calculated using a simple spin coupling model (Table 2) for $|S_{ad} = 7/2, S_{bc} = 3, S = \frac{1}{2}\rangle$.[6,9] Qualitatively this can be explained by the fact that in this case the S_b and S_c spins become parallel forming a $S_{bc} = 3$ pair and that the J_{ab} and J_{cd} antiferromagnetic couplings lead to a parallel ordering of spins a and d to give $S_{ad} = 7/2$. The S_{bc} spin is then antiparallel to the S_{ad} one to give a total $S = \frac{1}{2}$ (see Scheme 1 **B** above). This is one case where the simple spin coupling model holds for a linear tetramer.

Assuming Mn^{III} to be on site b we obtain Fig. 5(*b*). The value of the spin projection of Mn^{III} drops down quite significantly from +1 when an antiferromagnetic coupling is built between sites b and c; spin density goes from site b to sites c and d. Site d obtains even more spin density than site b. When $J_{bc} \gg 0$, the diagram corresponds to a $|S_{bc} = 7/2, S_{ad} = 3, S = \frac{1}{2}\rangle$ state.

Application to $[Mn^{III}Mn^{IV}{}_3O_6(bipy)_6]^{3+}$

The following point of the discussion will be devoted to the relation one can establish between the two sets of Mn indices, numbers 1–4 and letters a–d. In particular, a location for the Mn^{III} ion is proposed.

The spin projection absolute values estimated from the simulation correspond approximately to a large one with the three others close to half that value. First, we note that on every Mn atom the spin density is 'important' which means that strong magnetic connections are operative here and that indeed the tetranuclear structure is maintained under the conditions of our experiment. Secondly, we immediately see from Fig. 5(*a*) that these types of values are expected for a linear tetramer with Mn^{III} at one end (site a) and $J_{ab} = J_{bc} = J_{cd} < 0$.

More precisely we represented in Fig. 5 the experimental $\langle \boldsymbol{S}_{iz} \rangle$ values with a tolerance of 5%. This determines the position and width of four ribbons. In Fig. 5(*a*) we identify $J_{bc} = -0.64$ as a value which gives calculated $\langle \boldsymbol{S}_{iz} \rangle$ values in the range of the experimental values. In Fig. 5(*b*), one sees that no J_{bc} value gives comparable agreement.

Note also that a Mn^{III} ion in a terminal position (a or d) makes sense from a chemical point of view since the coordination sphere contains two oxygen and four nitrogen atoms compared to the N_2O_4 environment of site b (or c).

It is possible to refine the previous solution by allowing J_{ab} to vary (keeping $J_{cd} = -1$). We built a program which varies systematically J_{ab} and J_{bc} and computes the $\langle \boldsymbol{S}_{iz} \rangle$ and an agreement factor defined as $R = \Sigma_i |\langle \boldsymbol{S}_{iz} \rangle_{calc} - \langle \boldsymbol{S}_{iz} \rangle_{found}|$. The best solution was obtained for $J_{ab} = -1.15$ and $J_{bc} = -0.63$ with $\langle \boldsymbol{S}_{az} \rangle = +0.960$ (Mn^{III}, found +0.989), $\langle \boldsymbol{S}_{bz} \rangle = -0.500$ (found −0.521), $\langle \boldsymbol{S}_{cz} \rangle = +0.432$ (found +0.432), $\langle \boldsymbol{S}_{dz} \rangle = -0.393$ (found −0.392). The agreement is very satisfying and suggests that a reasonable description of the electronic structure of $[Mn_4O_6(bipy)_6]^{3+}$ is achieved. From magnetic susceptibility measurements on $[Mn_4O_6(bipy)_6]^{4+}$, $J_{ab} = J_{cd} = -1$ and $J_{bc} = -1.52$ (arbitrary units) were obtained. There seems to be here a discrepancy between both methods since one expects that reduction on center a must affect only J_{ab}. The J values obtained for $[Mn_4O_6(bipy)_6]^{3+}$ could be indicative that the Jahn–Teller distortion of $Mn_a{}^{III}$ influences $Mn_b{}^{IV}$ which leads to a change of J_{bc}. Another possibility would be that in order to get a fully coherent description between both oxidation states of the cluster, J_{ac} and J_{bd} constants need to be taken into account. This is mathematically feasible but we postpone this approach to later work.

Comparison with OEC

In Fig. 3, the multiline signal of OEC is compared to that of $[Mn_4O_6(bipy)_6]^{3+}$. The multiline X-band EPR signal has a

Table 3 Literature values of the hyperfine parameters of OEC

$\|A_1\|$ MHz	$\|A_2\|$ MHz	$\|A_3\|$ MHz	$\|A_4\|$ MHz	Ref.
369.0	262.9	242.5	232.3	6 (a)
366.9	261.4	244.6	57.3	(b)
277	277	226	250	11 (c)
363	363	288	226	
305.7*	305.7*	246.7*	242.0*	
280	257	237	237	(d)
300	337	237	237	
287.7*	283.7*	237*	237*	
271.4	243.1	229.0	217.7	8
252.2	252.2	252.2	252.2	19

* Isotropic average; values are presented in the decreasing order of isotropic averages. Simulations of Bonvoisin *et al.*[6] (a) and (b) have not been interpreted with a spin coupling model. Simulation of Zheng *et al.*[11] (c) has been interpreted as corresponding to a $|7/2,4,1/2\rangle$ state of a $Mn^{III}_3Mn^{IV}$ tetramer. Simulation of Zheng *et al.*[11] (d) has been interpreted as corresponding to a $|7/2,3,1/2\rangle$ state of a $Mn^{III}Mn^{IV}_3$ tetramer.

width of about 180 mT and contains 18 major lines plus one in the center of the spectrum and possible extra lines in the wing. Different simulations have been proposed (see Table 3).

We notice that the values are relatively different from one group to the other. Bonvoisin *et al.*[6] have proposed two simulations with isotropic parameters. One with a small $|A_4|$ has been discarded by ENDOR data. The other has a $|A_1|$ larger than in all other simulations. In fact we now have better simulations with a smaller $|A_1|$. The other simulations, as far as we know, have not been challenged although Belinskii[20] did not propose his values as adapted to a simulation but to general spin coupling considerations.

A clear difference between the parameters of Zheng and Dismukes[9] and those of Kusunoki[8] on one hand and those deduced here for $[Mn_4O_6(bipy)_6]^{3+}$ on the other is the absence in OEC of a large $|A_1|$ value.

A first possibility to explain this difference is that the redox states of $[Mn_4O_6(bipy)_6]^{3+}$ and OEC are different. Indeed Zheng and Dismukes[9] favoured a III_3,IV oxidation state for OEC. This is in contradiction with the conclusion drawn from XANES studies although the previous authors interestingly remark that five-co-ordinated Mn ions could present unusual X-ray absorption edges.

A second possibility is that the oxidation state in the S_2 state of OEC is indeed IV_3,II and that the difference between the EPR spectra of OEC and this model compound originates in a substantial structural difference between both clusters.

A third possibility is that the structural differences between $[Mn_4O_6(bipy)_6]^{4+}$ and OEC are subtle but change drastically the spectrum. Indeed $[Mn_4O_6(bipy)_6]^{4+}$ is topologically equivalent to Klein's proposal for OEC. Along this line of thought we can envision three causes for a change in the EPR spectrum. (*i*) Different values of the intrinsic hyperfine parameters due to local environments quite different to those in OEC.[9] (*ii*) A change in the location of Mn^{III}, central *versus* terminal. Recently Boussac *et al.*[21] showed that by near-infrared irradiation at 100 K the $g = 2$ multiline signal is converted into the $g = 4.1$ signal. They proposed the translocation of the +III oxidation state from one Mn site to another as the origin of this effect. (*iii*) Different J_{ij} coupling parameters in OEC and in the model complex. To answer these questions, new model complexes will certainly help and are valuable synthetic targets. We are also currently applying to the EPR spectra of OEC the strategy we successfully tested here for $[Mn_4O_6(bipy)_6]^{3+}$.

Conclusion

γ-Radiolysis has been used to obtain mixed-valence states ($Mn^{III}Mn^{IV}$) of Mn clusters. The procedure has been checked with the generation of $[Mn^{III,IV}_2O_2(phen)_4]^{3+}$. The same procedure has allowed the formation of $[Mn^{III}Mn^{IV}_3O_6(bipy)_6]^{3+}$ starting from the well characterized $[Mn^{IV}_4O_6(bipy)_6]^{4+}$ tetramer. The X-band EPR spectrum of $[Mn^{III}Mn^{IV}_3O_6(bipy)_6]^{3+}$ has been recorded. It constitutes the first example of an artificial $Mn^{III}Mn^{IV}$ tetramer with a $S = \frac{1}{2}$ ground state. This spectrum has been simulated in different approximations. The best simulation was obtained for a full set of rhombic tensors. The isotropic parts of the ^{55}Mn hyperfine couplings have been found equal to $|A_1| = 449.2$ MHz, $|A_2| = 228.3$ MHz, $|A_3| = 189.4$ MHz, $|A_4| = 171.5$ MHz. One pair is strongly reminiscent of the $[Mn_2O_2(bipy)_4]^{3+}$ pair with $|A_1| = 453$ MHz, $|A_2|$ 218.7 MHz.[11] The center with the largest hyperfine coupling has a large anisotropy, the others being almost isotropic. This identifies it as a Mn^{III} high-spin ion. Using intrinsic hyperfine parameters of the $[Mn_2O_2(bipy)_4]^{3+}$ dinuclear system, absolute values of spin projections $\langle \boldsymbol{S}_{iz} \rangle$ were determined for $[Mn^{III}Mn^{IV}_3O_6(bipy)_6]^{3+}$. Using the criterion $\Sigma_i \langle \boldsymbol{S}_{iz} \rangle = 0.5$, a unique distribution of signs for the $\langle \boldsymbol{S}_{iz} \rangle$ was obtained. These values were then interpreted with a three J linear spin coupling model with Mn^{III} at a terminal site ($J_{ab} = -1.15$, $J_{bc} = -0.64$, $J_{cd} = -1$ in arbitrary units). Comparison with OEC shows that hyperfine couplings in OEC are less dispersed in absolute values than in this model complex. Future work will be devoted to an ^{55}Mn ENDOR study of this model to ascertain the hyperfine coupling parameters. A similar interpretative procedure is currently being applied to the EPR spectrum of OEC.

Acknowledgements

This research was supported by the European community through the Training and Mobility of Researchers 'Ru–Mn Artificial Photosynthesis' network.

References

1 V. K. Yachandra, K. Sauer and M. P. Klein, *Chem. Rev.*, 1996, **96**, 2927.
2 R. D. Guiles, J.-L. Zimmermann, A. E. McDermott, V. K. Yachandra, J. L. Cole, S. L. Deixheimer, R. D. Britt, K. Weighardt, U. Bossek, K. Sauer and M. P. Klein, *Biochemistry*, 1990, **29**, 471.
3 J. Messinger, M. Badger and T. Wydrzynski, *Proc. Natl. Acad. Sci. USA*, 1995, **92**, 3209.
4 C. Tommos, X.-S. Tang, K. Warncke, C. W. Hoganson, S. Styring, J. McCracken, B. A. Diner and G. T. Babcock, *J. Am. Chem. Soc.*, 1995, **117**, 10 325; M. T. Caudle and V. L. Pecoraro, *J. Am. Chem. Soc.*, 1997, **119**, 3415.
5 G. C. Dismukes and Y. Siderer, *Proc. Natl. Acad. Sci. USA*, 1981, **78**, 274.
6 J. Bonvoisin, G. Blondin, J.-J. Girerd and J.-L. Zimmermann, *Biophys. J.*, 1992, **61**, 1076.
7 K. A. Åhrling and R. J. Pace, *Biophys. J.*, 1995, **68**, 2081.
8 M. Kusunoki, *Chem. Phys. Lett.*, 1992, **197**, 108.
9 M. Zheng and G. C. Dismukes, *Inorg. Chem.*, 1996, **35**, 3307.
10 D. W. Randall, B. E. Sturgeon, J. A. Ball, G. A. Lorigan, M. K. Chan, M. P. Klein, W. H. Armstrong and R. D. Britt, *J. Am. Chem. Soc.*, 1995, **117**, 11 780.
11 M. Zheng, S. V. Khangulov, G. C. Dismukes and V. V. Barynin, *Inorg. Chem.*, 1994, **33**, 382.
12 Y.-M. Frapart, A. Boussac, R. Albach, E. Anxolabéhère-Mallart, M. Delroisse, J.-B. Verlhac, G. Blondin, J.-J. Girerd, J. Guilhem, M. Césario, A. W. Rutherford and D. Lexa, *J. Am. Chem. Soc.*, 1996, **118**, 2669.
13 R. Davydov, *J. Am. Chem. Soc.*, 1994, **116**, 11 120.
14 H. A. Goodwin and R. N. Sylva, *Aust. J. Chem.*, 1967, **20**, 629.
15 C. Philouze, G. Blondin, J.-J. Girerd, J. Guilhem, C. Pascard and D. Lexa, *J. Am. Chem. Soc.*, 1994, **116**, 8557.
16 S. R. Cooper and M. Calvin, *J. Am. Chem. Soc.*, 1997, **99**, 6623.
17 A. L. Nivorozhkin, E. Anxolabéhère-Mallart, P. Mialane, R. Davydov, J. Guilhem, M. Césario, J.-P. Audière, J.-J. Girerd, S. Styring, L. Schussler and J.-L. Seris, *Inorg. Chem.*, 1997, **36**, 846.
18 V. K. Yachandra, V. J. DeRose, M. J. Latimer, I. Mukerji, K. Sauer and M. P. Klein, *Science*, 1993, **260**, 675.
19 M. Weissbluth, in *Atoms and molecules*, Academic Press, New York, London, Student Edition, 1978.
20 M. I. Belinskii, *Chem. Phys.*, 1994, **179**, 1.
21 A. Boussac, J.-J. Girerd and A. W. Rutherford, *Biochemistry*, 1996, **35**, 6984.

Received 15*th May* 1997; *Paper* 7/03381H